Morphostructural Zonation and Preliminary Recognition of Seismogenic Nodes Around the Adria Margin in Peninsular Italy and Sicily

A.I. Gorshkov[1,2], G.F. Panza[2,3], A.A. Soloviev[1,2], and A. Aoudia[2,3]

1. International Institue of Earthquake Prediction Theory and Mathematical Geophysics, Russian Academy of Sciences, Moscow, Russia, email: gorshkov@mitp.ru
2. The Abdus Salam International Center for Theoretical Physics, Trieste, Italy, email: panza@dst.univ.trieste.it
3. Department of Earth Sciences, University of Trieste, Italy

ABSTRACT: *The study is based on the assumption that strong earthquakes are associated with the nodes that are specific structures formed around the intersections of the fault zones. The nodes have been delineated with the morphostructural zonation method, based on the idea that the lithosphere is made-up of different-scale blocks, separated by mobile boundaries. The morphostructural map, compiled with the GIS technology at the scale of 1:1,000,000, shows the hierarchical block-structure of the region, the network of boundary zones, the bounding blocks, and the loci of the nodes. The results of the morphostructural analysis indicate the very important role of the E-W trending fault zones in the present-day block-structure of the region around the Adria margin, peninsular Italy and Sicily, especially in the Apennines. The crustal earthquakes with $M \geq 6.0$ recorded in the region are nucleated at some of the mapped nodes. With the assumption that the future strong events will occur at the nodes, the seismic potential of each node has been evaluated for two magnitude thresholds, $M \geq 6.0$ and $M \geq 6.5$. The pattern recognition algorithm "CORA-3" has been used in order to identify the nodes capable of earthquakes with $M \geq 6.0$. Due to the few recorded quakes with $M \geq 6.5$ in the studied region, pattern recognition is not applicable to identify the nodes prone to quakes with $M \geq 6.5$. The nodes capable of such earthquakes have been identified by the criteria of high seismicity nodes, previously derived from pattern recognition in the Pamirs-Tien Shan region. The results obtained indicate a high seismic potential for the studied area and provide important information for seismic hazard assessment: a number of nodes where strong events have not been recorded to date, have been recognized to be prone to large earthquakes and they may warrant a detailed interdisciplinary investigation.*

Keywords: Seismogenic nodes; Morphostructural zonation; Pattern recognition; Adria margin

1. Introduction

The Adria plate, delineated by Lort [1] and carefully studied by Anderson & Jackson [2], is positioned in the central part of the Mediterranean and it is surrounded by high-topographic belts that mark its boundaries. The seismicity pattern exhibits the increase of the seismic activity and of the intensity of single events from the Adriatic Sea, central part of the plate, toward its margins. The territories around the Adria plate are densely populated and industrialized. The goal of the planned investigation is to identify the areas of high seismic potential along the margins of the Adria. Here we deal with the region comprising the Italian Peninsula, Sicily and the adjacent marine shelf of the Tyrrhenian and Adriatic seas.

The studied area is a well-defined seismo-active region frequently affected by strong earthquakes. Seismic

hazard assessment and identification of the seismogenic zones in this region have been the subject of numerous investigations in the last decades e.g. [3, 4, 5, 6, 7 and 8].

This study is based on the assumption that strong earthquakes are associated with the nodes, specific structures that are formed around the intersections of the fault zones. The fact that earthquakes are nucleated at the nodes was first established from observations in the Pamirs and Tien Shan [9]. The non-random nature of this phenomenon has been proven by an especially designed statistical test [10]. McKenzie & Morgan [11] first described the physical mechanism of node's formation, and the model for their origin has been recently proposed by Gabrielov, et al [12]. According to this model, the block interaction along intersection faults leads to stress and strain accumulation and secondary faulting around the intersection. This causes the generation of new faults of progressively smaller size, so that a hierarchical mosaic structure- a node - is formed around the intersection.

The nodes are delineated by the morphostructural zonation method [13, 14] on the basis of geomorphologic and tectonic information, with no any connection with seismicity data. The nodes prone to strong earthquakes are identified by the methodology based on pattern recognition [9]. This approach has been applied to many regions of the world for the recognition of earthquake-prone areas [3, 9, 15, 16, 17, 18, 19, 20, 21], and the predictions made by this methodology in the last 3 decades have been followed by many events (84% of the total) that occurred in some of the nodes previously recognized to be the potential sites for the occurrence of strong events [22, 23].

In this study we recognize seismogenic nodes for two magnitude thresholds, $M \geq 6.0$ and $M \geq 6.5$.

Pattern recognition is used to identify the nodes capable of earthquakes with $M \geq 6.0$, as done earlier by Caputo et al [3] for the Italian territory. The update of Caputo et al [3] investigation is made necessary by two main of reasons;

- The new data about active faults, geotectonics and seismotectonics of Italy, become available during the last two decades and
- The availability of reconsidered and updated earthquake catalogues of Italy. This study is performed on a more detailed level (morphostructural zonation performed at the scale of 1:1,000,000) than the one by Caputo et al [3] and gravity data are used in the recognition of the nodes prone to earthquakes with $M \geq 6.0$.

In the studied region, pattern recognition is not applicable to identify the nodes prone to $M \geq 6.5$ earthquakes because the number of such events is insufficient for the learning stage of the pattern recognition. Because of this, in order to identify the nodes prone to the $M \geq 6.5$ quakes, we use the criteria of high seismicity ($M \geq 6.5$) defined by pattern recognition in the Tien Shan-Pamirs region [24]. The criteria have been already tested in other parts of the Apline-Himalayan seismic belt, namely in the Greater Caucasus [19], in the Carpatho-Balkan mountains [25] and in the Kopet Dagh region [26]. In all these regions, the nodes hosting $M \geq 6.5$ quakes were properly recognized.

2. Methodology

Two principal steps compose the methodology. In the first step, the subjects of the analysis-the morphostructural nodes- are delineated by the morphostructural zonation method. In the second one, the seismic potential of each node is evaluated with the help of the pattern recognition algorithm "*CORA*-3". Hereby we report only the basic definitions necessary to facilitate the reading of the paper.

2.1. Identification of the Nodes

The nodes are delineated by means of the methodology called morphostructural zonation (*MZ*), which is based on the widely accepted concept that the lithosphere is built up by different-scale blocks separated by mobile boundaries. Special attention is paid to the present-day topography, a clear expression of the recent tectonics.

By the *MZ* the territory is divided into a system of hierarchically ordered areas, characterized by certain homogeneity of the present-day topography and of the tectonic structure. Three types of morphostructures are distinguished by *MZ:*

- Areas (block) of different ranks;
- Their boundary zones, called lineaments;
- Sites where boundary zones intersect, called nodes.

The present-day topography is chiefly analyzed in terms of its morphometry, and the following topographic features are taken into consideration

- Elevation, orientation, and slope of topography;
- The drainage pattern and its variations;
- Linear elements of the Earth surface such as rectilinear segments of rivers, ravines, escarpments, etc.

MZ is hierarchically ordered, hence the territorial units (blocks) and the boundary zones are assigned with ranks. The regional structures with a common orogenesis (e.g., the Apennines as a whole) are considered as the highest (first) rank units; in *MZ* they are called *mountain countries*. They are divided into second rank areas called *megablocks*. The megablocks are further subdivided into areas of third rank called blocks. The neighboring blocks should differ at least in one of the three considered characteristics of the present-day topography. The megablocks are the territories within which all the three features of the present-day topography are similar or change with a common regularity.

A boundary zone is of first, second or third rank, if it limits first- or second - or third-rank areas, respectively. With respect to the regional trend of the tectonic structure and topography, two types of boundary zones are distinguished;

- ❖ Longitudinal and
- ❖ Transverse lineaments

Longitudinal lineaments are approximately parallel to the regional strike of the tectonic structure and of the topography and include long pieces of the prominent faults. Transverse lineaments intersect the regional trend of the tectonic structure and of the topography. They appear on the Earth' surface discontinuously and are represented by tectonic escarpments, by rectilinear parts of river valleys, and partly by faults.

The nodes are formed at the sites where the block boundaries of different orientation intersected, and are characterized by particularly increased fragmentation of the crust and contrasting geotectonic movements with a resulting mosaic pattern of the tectonic structure and of the topography.

2.2. Recognition of Seismogenic Nodes

In the framework of our methodology, the problem of pattern recognition is formulated as follows. Given a set of patterns each of them belongs to one and only one of a few classes. This general set of patterns contains some sample patterns ("*training set*") whose classification is a *priori* known. The goal is to select the *distinctive features* of each class and, using these features, to classify all incoming patterns.

In our case, each pattern is a node represented by a vector. The components of each vector are measured values of the parameters of the nodes. This parameter vector is exploited as an input of a classifier.

The identification of earthquake-prone areas is a two-class recognition problem since any node is either prone or non-prone to an earthquake wit a certain magnitude. The goal of pattern recognition is to divide all the nodes delineated in the studied region in the two classes:

i Class D, constituted by the nodes where strong earthquakes may be nucleated (hosted);

ii Class N, constituted by the nodes not capable of strong earthquakes.

The recognition process includes two stages:

1. *Learning stage:*
Selection of the distinctive features of each class on the basis of the training set composed by D_0 and N_0 subsets, which are constituted by all the sample nodes representative of the classes D and N, respectively.

2. *Classification stage*:
Determination of which class each node belongs to.

The well-tested "*CORA*-3" pattern recognition algorithm, described by Gelfand et al [17] and Cisternas et al [16] has been used in this work. The distinctive features (characteristic traits) for classes D and N are selected as follows.

Let l be the number of components of the binary vectors representing the node. The trait is a matrix A defined as follows:

$$A = \begin{Vmatrix} i_1 & i_2 & i_3 \\ \delta_1 & \delta_2 & \delta_3 \end{Vmatrix},$$

where i_1, i_2, i_3, are natural numbers, such that $1 \le i_1 \le i_2 \le i_3 \le l$ and $\delta_1, \delta_2, \delta_3$ are equal to 0 or to 1. We say the node (binary vector) numbered i, $\omega^i = (\omega_1^i, \omega_2^i, ..., \omega_l^i)$ has the trait A if

$$\omega_{i_1}^i = \delta_1,\ \omega_{i_2}^i = \delta_2,\ \omega_{i_3}^i = \delta_3.$$

The characteristic traits are selected by using four parameters of the algorithm $k_1, \bar{k}_1, k_2, \bar{k}_2$, which must be integer non-negative values. Let W be the set of all the nodes considered and $K(W, A)$ the number of nodes $\omega^i \in W$, which have the trait A. The trait A is a characteristic trait of class D if $K(D_0, A) \ge k_1$ and $K(N_0, A) \le \bar{k}_1$, and the trait A is a characteristic trait of class N if $K(N_0, A) \ge k_2$ and $K(D_0, A) \le \bar{k}_2$.

The classification is made as follows. For each node ω^i the number ${n_D}^i$ of the characteristic traits of class D, the number ${n_N}^i$ of the ones of class N, and the difference $\Delta_i = {n_D}^i - {n_N}^i$ are calculated. Set D includes the nodes ω^i, for which $\Delta_i \ge \Delta$. The nodes, for which $\Delta_i < \Delta$, are assigned to set N. Δ, as well as $k_1, \bar{k}_1, k_2$, and $\bar{k}_2$ is a parameter of the algorithm.

Since the "*CORA*-3" algorithm works with binary vectors, it is necessary to convert the vectors describing the nodes (actual values of the parameters) into binary vectors by means of discretization and *coding*. The range of the value of each parameter is divided into two or three parts (interval open to the left) by specifying one or two thresholds of discretization. This leads to the loss of some information but it makes the results of the recognition more stable to the fluctuations in the data, e.g. the non-uniqueness of the *MZ*. In one-threshold discretization two intervals are considered for the real component, which is converted into one binary component with the value 1 ("small") or 0 ("large"). Correspondingly, in two-threshold discretization the real component is converted into two binary components with the values 11 ("small"), 01 ("medium") or 00 ("large").

3. Morphostructural Zonation

The morphostructural map, shown in Figure (1), has been implied using the *GIS* technology at the scale of 1:1:000,000

by the combined analysis of topographic, tectonic, geological maps and satellite photos. The designed map shows the hierarchical block-structure, the network of the lineaments bounding the different blocks, and the loci of the nodes-sites where lineaments intersect.

The considered part of the Adria plate includes most of the Italian Peninsula and the adjacent marine shelf. The large-scale tectonic domains that build up the region have been assigned to the first-rank areas. They are the Apennines, Calabria and Sicily, which differ in present-day topography (physiography), tectonic style, lithology (stratigraphy), and geological history.

3.1. Apennines

Their borders are the Alps and the Tyrrhenian basin to the west, the Po basin and the Adriatic-Apulian foreland to the north and to the east, and Calabria to the south.

3.1.1. First-Rank Lineaments

The lineament 1-7, see Figure (1), corresponding to the Sestri-Voltaggio fault zone [27], is the boundary between the Apennines and the western Alps. In the north and in the east, the lineament 1-98, that separates the Apennines from the Adriatic foreland, it has been traced along the footline of the Apennines, therefore its position and configuration are slightly different from the fault line marking the Apennine-Maghrebides Main Thrust Front [28]. In the south, the lineament 103-106 is the boundary between the Appennines and Calabria: it corresponds to the Sangineto line [29] or to the Palinuro fault according to Mantovani et al [30]. In the west, the junction of the Apenninic structures with the Corsica-Sardinia block and

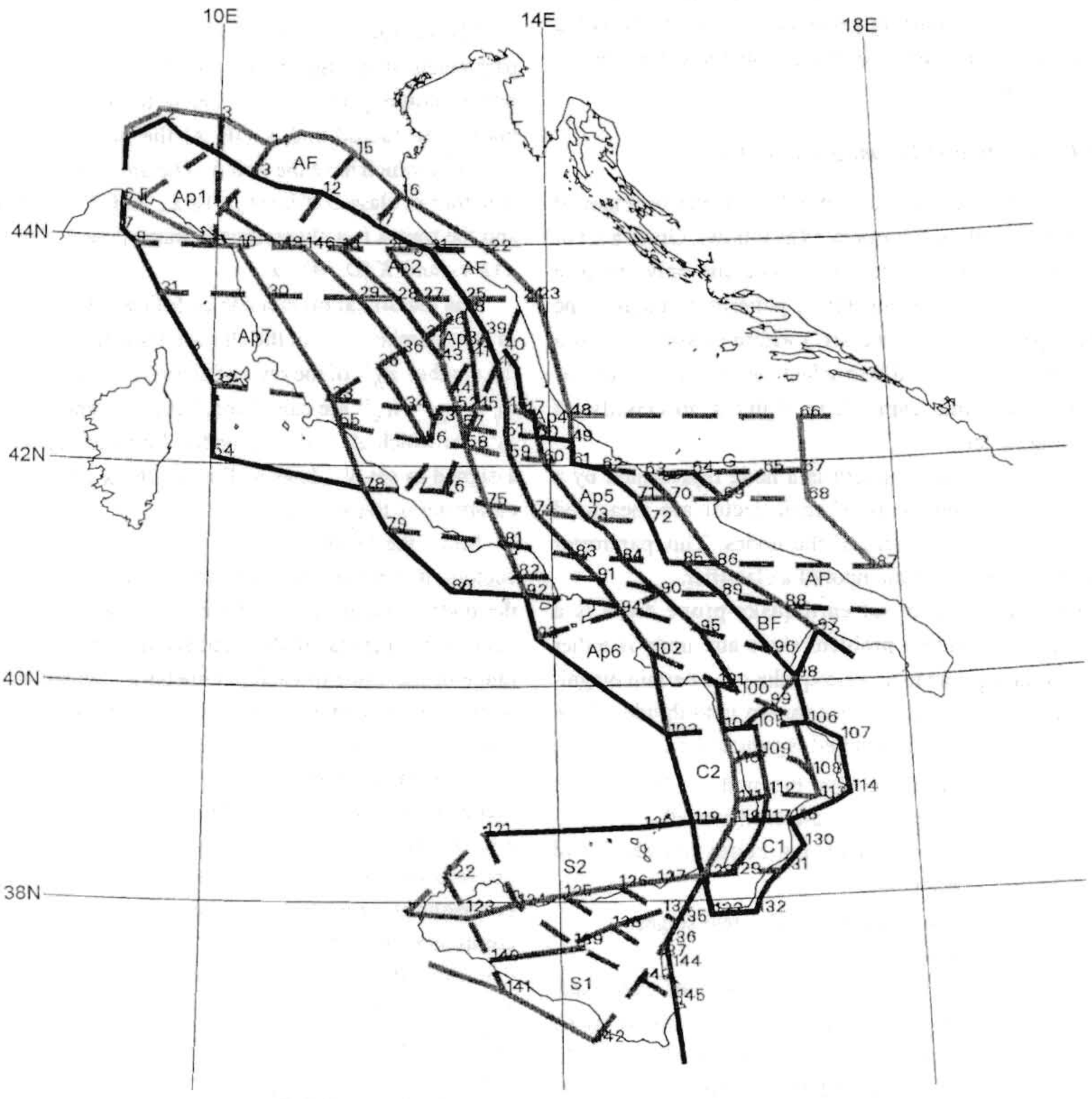

Figure 1. Morphostructural map of the study area. Violet lines are the lineaments of the first rank, blue lines are the lineaments of the second rank, green lines are the lineaments of the third rank, continuous lines are the longitudinal lineaments, discontinuous ones are the transverse lineaments. Nodes are numbered from 1 to 146. *Ap*, Apennines; *AF*, Adriatic foredeep; *AP*, Apulian platform; *BF*, Bradanic foredeep; *C*, Calabria; *G*, Gargano Promontory; *S*, Sicily.

the Tyrrhenian basin is very complex. The lineament 7-103, marking this boundary, has been traced along the steep slope between the shelf zone and the abyssal plains of the Tyrrhenian basin. Some fragments of the lineament include faults shown on tectonic maps [28, 31].

3.1.2. Megablocks and Lineaments of the Second Rank

Along the Apennines the topography changes sharply over short distances and this indicates that very inhomogeneous and complex recent tectonic movements are acting along the mountain chain. Due to the variety of its topography, seven megablocks have been outlined in the Apennines.

Megablock *Ap1*, see Figure (1), embraces the Northern Apennines comprising three en-echelon ridges. The megablock is divided into blocks by *NE -SE* transverse third-rank lineaments. Blocks differ in the height of topography and orientation of ranges. Their boundaries, transverse lineaments 8-13, 12-19 and 17-18, coincide with the transfer zones shown on the structural map of Carmignani et al [32].

In the Central Apennines, the megablocks *Ap*2, *Ap*3, *Ap*4 and *Ap*5 have been delineated. They differ in the dominant orientation, in the elevation of the mountain belt and they are separated by second-rank transverse lineaments with a near *E-W* trend. The important role of the *E-W* lineaments in the morphostructure of the Central Apennines is one of the main results of this study. In the previous version of the morphostructural map of Italy [3] only the lineament 8-21 was shown, and according to Philip [33], the Ancona-Anzio line is the most important orthogonal discontinuity in the Central Apennines. This line is shown on our morphostructural map as the third-rank lineament 24-76, which controls a local change of elevation of the Roman Apennines.

The lineaments 8-21 and 23-29 appear to be very important structural boundaries between the Northern and the Central Apennines (or even perhaps between the "fast moving" peninsula and the "slow moving" mainland north of 44^0 of latitude). The axes of the ridges, located northward and southward of this boundary, are remarkably shifted eastward suggesting left-lateral displacements along the lineament. Additionally, the strike of the eastern footline of the Apennines and of the Adriatic foredeep changes sharply at the intersection with this lineament. To the north and to the south of the lineament, contours of gravity anomalies [34, 35] and of the Moho discontinuity [36] display different pattern, indicating deep-seated deformations within the zone of the lineament. The deformations probably reach the upper mantle as indicated by the properties of the upper lithosphere (the lid), which exhibit a notable difference in areas separated by this lineament [37, 38].

The *E-W* trending lineament 23-29 limits to the north the Umbria-Marche Apennines. Wise et al [39] has identified, in this area, topographic lineaments with such orientation. The lineament is traceable to the east since the orientation of the fault system in the North Adriatic Sea floor changes from a *NNW* trend, north of the lineament, to a *WNW* trend south of it.

The lineament 47-52 is the northern boundary of the most elevated segment of the Apennines, the Gran Sasso Mountain; it includes the *E -W* Gran Sasso Front and an active fault bordering the Rieti basin [40]. The eastward extension of the lineament separates the shallow North Adriatic basin and follows the trend of the faults shown on the tectonic maps [28, 31].

The *E-W* lineament 58-62 delimits the Abruzzo Apennines; it is traced along the northern border of the Fucino Quaternary basin and it includes the Velino-Magnola Mts. fault [41]. Its eastern extension, the third-rank lineament 62-67, limits the Gargano Promoutary to the north.

We consider the nearly *E -W* lineament 72-75 as a morphostructural boundary between the Central and Southern Apennines. From the *MZ* point of view, the Ortona-Roccamonfina line [e.g. 8, 30] does not satisfy the requirements of a morphostructural boundary because south of the line the topography exhibits the same trend and elevation as the Central Apennines. In our opinion, a sharp change of the topography pattern is associated with the lineament 72-75. The zone of this lineament includes the nearly *E -W* left-lateral strike-slip motion identified by Salvini [42] near the town of Frosinone and a system of young Quaternary intermountain basins.

In the Southern Apennines, megablock *Ap*6, the topography is quite different from that in the Central Apennines that are formed mainly by hills and small ridges of chaotic orientation. The blocks, delineated by *MZ*, mostly differ in the topography elevation and are bounded by a system of nearly *E -W* transverse lineaments partly associated with faults. In particular, the lineament 82-89 near to the town of Avellino, includes an active fault defined by Bousquet et al [43] who suggest the widespread development, in the Southern Apennines, of seismogenic structures oriented *E -W*. The lineament 92-96 in the Southern Apennines includes faults shown on the structural map of Italy [28] and it is traceable, for a long distance, towards to the Corsica coastline in accordance with the magnetic lineament defined by Marson et al [38] within the Tyrrhenian Sea. The lineament 102-106 corresponds to the Pollino fault [44].

Unlike other segments of the Apennines, low topography and young volcanic activity characterize the megablock *Ap*7. The megablock is separated from the high-topographic belt by the second-rank lineament 19-92 which passes along the western footline of the Apenninic

ranges, in accord with the fault system shown on the structural and neotectonic maps [28, 45].

The morphostructural analysis of the Apennines tentatively indicates left-lateral motion along most of the outlined *E-W* transverse lineaments. This motion is evidenced in the topography by the eastward displacement of the range axes and of the eastern footline of the Apennines. These displacements led to situation that a block, located south of each lineament, is slightly shifted eastward with respect to those situated north of the same lineament. Of course, this is only a hypothesis on possible recent kinematics of the Apennines and a more accurate analysis has to be conducted.

3.2. Calabria

Unlike the Apennines and Sicily, crystalline rocks compose most of this mountain country, and the topographic pattern is markedly different as compared to the neighboring mountain countries.

3.2.1. First-Rank Lineaments

To the west and to the east, these lineaments are traced along steep scarps flanking the deep marine basins. The first-rank lineament 128-145 following the Messina-Giardini fault and the Malta Escarpment separates Calabria from Sicily.

3.2.2. Megablocks and Lineaments of the Second Rank

Two megablocks, marked *C*1 and *C*2 in Figure (1), have been delineated in the region. The first one occupies the peninsular part of Calabria, the second one embraces the adjacent shelf of the Tyrrhenian Sea. The two megablocks are separated by a longitudinal second-rank lineament traced along the steep fault scarp between the shelf and Calabria.

In Calabria, the structural setting is well evidenced by the regional morphology. All the outlined transverse third-rank lineaments are in agreement with the morphostectonic lines shown by Moretti & Guerra [46]. The dense network of lineaments is conditioned by the increased fragmention of the crust in this region.

3.3. Sicily

The topography and the structural setting of Sicily are clearly different as compared to the Apennines and Calabria. Low-elevated ranges with nearly *E-W* orientation and hills dominate the present-day surface relief.

3.3.1. First-Rank Lineaments

Sicily is bounded by first-rank lineaments only to the north and to the east since the western and southern morphostructural boundaries of this first-rank block are outside the region considered. The northern boundary, first rank lineament 119-121, is traced along the Aeolian and Ustica Island. To the west and to the south, Sicily is bounded by second-rank lineaments that separate the island from the shelf zone.

3.3.2. Megablocks and Lineaments of the Second Rank

Two megablocks, *S1* and *S2*, are delineated by *MZ*. Megablock *S1* occupied most of the island, while megablock *S2* includes the adjacent shelf zone. The boundary between them, lineament 123-128, is traced in accordance with the fault zone shown on the neotectonic map of Italy [45].

The third-rank longitudinal lineament 134-140 delimits the Kumeta-Alcantara Mountains. Transverse third-rank lineaments with *NW-SE* orientation are associated with the sharp changes of altitude of these mountains. The transverse lineaments 122-141 and 136-142 correspond to the Sciacca and the Comiso-Scicli faults [30], respectively.

3.4. Adriatic Foreland

The western edge of the Adriatic foreland along the Apennines is marked on the morphostructural map by the second-rank lineaments 1-49 and 70-97, the eastern boundaries of the Adriatic (*AF*) and Bradanic (*BF*) foredeeps, respectively. These lineaments are traced in accord with the faults shown on the neotectonic map of Italy by Ambrosetti et al [45]. The Apulian platform (*AP*) is bounded by the second-rank lineaments 70-97, 70-68, and 68-87. The Gargano promontory (*G*) is delimited by the lineaments corresponding to the high gradient zones of horizontal isostatic anomalies [37] and to well recognized active faults e.g. [8, 30, 45].

4. Nodes and Seismicity

Since the nodes have been outlined on the basis of cartographic sources without field investigations, their natural boundaries have not been defined. From observations in the Pamirs-Tien Shan region [14] the node dimensions have been established to be 40-60*km* in length and 30-40*km* in width. In this work the nodes are defined as a circle of 25*km* radius surrounding each point of intersection of lineaments. Such node dimension is comparable with the size of the earthquake source for the magnitude range considered in this work, since, a ccording to Riznichenko [47] and Wells & Coppersmith [48], the source size of an earthquake with $M = 6.0$ is about 20*km* in length and about 10*km* in width.

Using this formal node definition, each point of lineament intersection is a node but in reality, two or three closely situated intersections may belong to the same node.

In order to evaluate the correlation between the

nodes and the $M \geq 6.0$ quakes recorded in the region, we used two earthquake catalogues *NT* 4.1.1. [49] and *CCI*-1996 [50], covering the entire region and containing events from 1000 to 1997. Although these catalogues sometimes exhibit different values for the same parameters (mainly magnitude) for the same events, they are the most complete sources on the seismic history of Italy. Table (1) contains the list of the nodes and of the earthquakes falling within each of them. The parameters of the earthquakes (location and magnitude) are those listed in the two used catalogues. The epicenters of the selected events are slightly different in the two catalogues, and to plot them on the morphostructural map, see Figure (2), we arbitrarily used the coordinates given by the *NT*4.1.1. catalogue. Figure (2) shows only the events classified with $M \geq 6.0$ in both catalogues.

The epicenters of these earthquakes are located near to the intersection of lineaments. With the only two exceptions of the epicenter of the 1688 earthquake, located near node 73, and the epicenter of the 1732 earthquake, located between the nodes 84-85-90, the distance between the epicenters and the points of intersection does not exceed 25*km* (Table (1) Figure (2)). Thus it is possible to apply pattern recognition for the node classification.

5. Identification of the Seismogenic Nodes

The seismic potential of the delineated nodes has been evaluated for two magnitude thresholds, $M \geq 6.0$ and $M \geq 6.5$. The nodes prone to earthquake with $M \geq 6.0$ are identified with the pattern recognition algorithm "*CORA*-3" applied to the earthquake-prone areas determination for the first time by Gelfand et al [9]. The nodes with larger

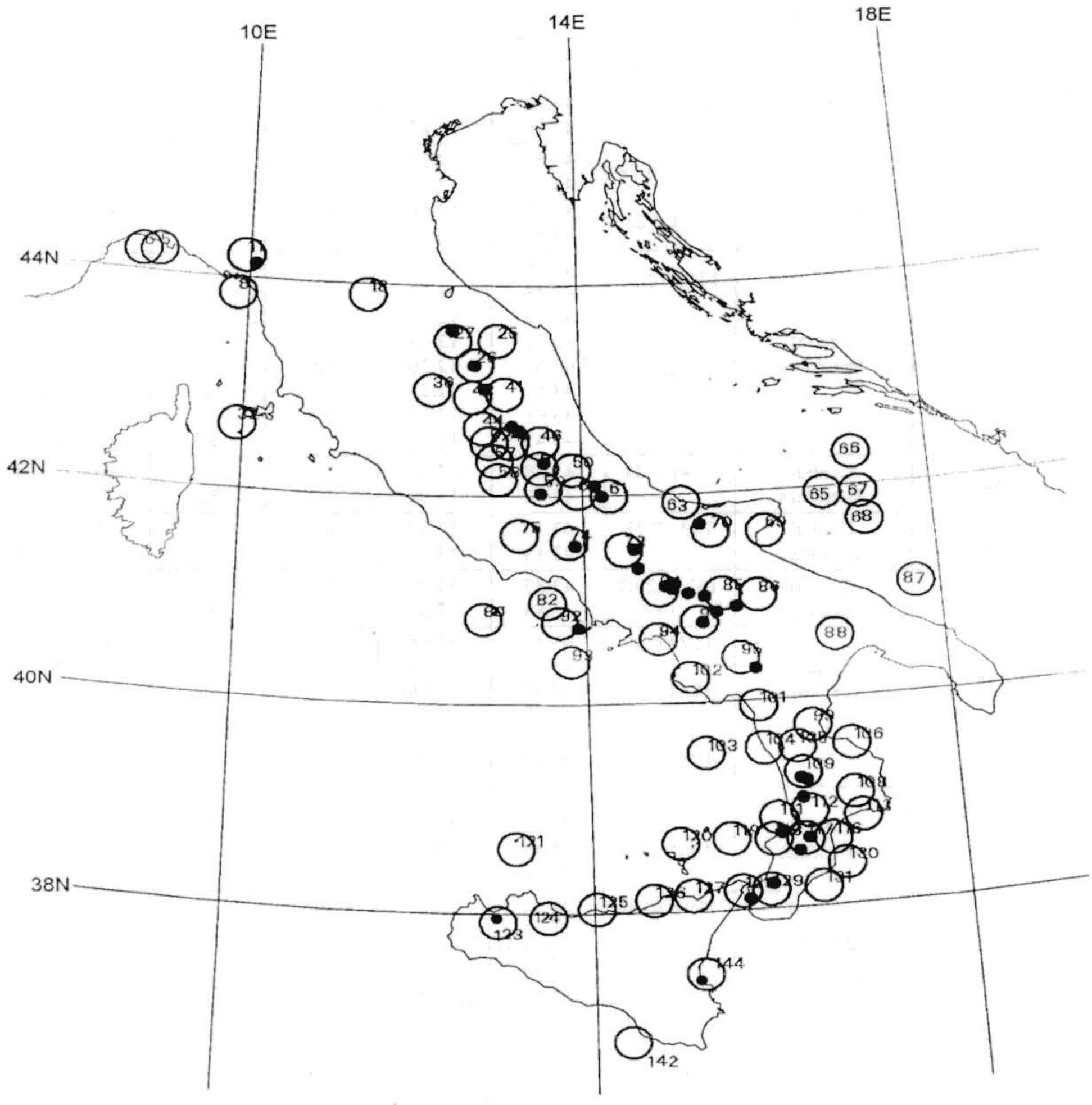

Figure 2. Result of the recognition of the nodes prone to earthquakes with $M \geq 6.0$. Dots are the epicenters with $M \geq 6.0$ listed in Table (1). Circles are the nodes recognized to be prone to earthquakes with $M \geq 6.0$. Numbering of nodes as in Table (4).

Table 1. Earthquakes with $M \geq 6.5$.

Node Number	Region	Earthquakes Date	Lat N	Lon E	M_s**	M_l	References
11*	North Apennines	1920.9.07	44.20	10.20	6.5		NT4.1.1
			44.20	10.25		6.7	CCI-1996
17	North Apennines	1688.4.11	44.40	11.97	6.2		NT4.1.1
			44.38	11.92		5.2	CCI-1996
		1781.4.04	44.23	11.75	6.2		NT4.1.1
			44.23	11.80		5.4	CCI-1996
		1661.3.22	44.03	11.90	6.2		NT4.1.1
			44.03	11.95		5.7	CCI-1996
18	Central Apennines	1919.6.29	43.95	11.48	6.3		NT4.1.1
			43.95	11.48		5.6	CCI-1996
		1542.6.13	44.00	11.40	6.2		NT4.1.1
			44.00	11.35		5.7	CCI-1996
20	Central Apennines	1584.9.12	43.93	11.93	6.2		NT4.1.1
		9.10	43.83	12.00		5.1	CCI-1996
21	North Apennines	1916.5.17	43.93	12.68	6.0		NT4.1.1
			44.17	12.92		4.7	CCI-1996
25	Central Apennines	1930.10.30	43.63	13.33	6.0		NT4.1.1
			43.67	13.27		5.9	CCI-1996
26*	Central Apennines	1751.7.27	43.25	12.75	6.7		NT4.1.1
			43.23	12.75		6.1	CCI-1996
		1747.4.17	43.20	12.82	6.2		NT4.1.1
			43.20	12.83		5.1	CCI-1996
27*	Central Apennines	1389.10.18	43.53	12.35	6.2		NT4.1.1
			43.50	12.25		5.1	CCI-1996
		1781.6.03	43.58	12.50	6.4		NT4.1.1
			43.58	12.57		6.3	CCI-1996
28	Central Apennines	1352.12.25	43.48	12.13	6.2		NT4.1.1
			43.48	12.15		5.1	CCI-1996
		1458.4.26	43.45	12.23	6.2		NT4.1.1
			43.52	12.18		5.1	CCI-1996
		1789.9.30	43.52	12.20	5.9		NT4.1.1
			43.52	12.23		6.3	CCI-1996
		1917.4.26	43.48	12.12	5.9		NT4.1.1
			43.47	12.12		6.3	CCI-1996
38	Central Apennines	1741.4.24	43.38	12.98	6.2		NT4.1.1
			43.42	13.00		5.6	CCI-1996
39	Central Apennines	1799.7.28	43.17	13.17	6.2		NT4.1.1
			43.13	13.13		5.6	CCI-1996
41	Central Apennines	1328.12.01	42.87	13.00	6.7		NT4.1.1
		12.04	42.85	13.02		5.6	CCI-1996
43*	Central Apennines	1279.4.30	43.10	12.90	6.7		NT4.1.1
			43.27	12.78		5.6	CCI-1996
		1832.1.13	42.95	12.60	5.9		NT4.1.1
			42.98	12.60		6.8	CCI-1996
		1997.9.26	43.02	12.87	6.1 (mb)		NEIC (GHDB)
45*	Central Apennines	1639.10.07	42.63	13.25	6.7		NT4.1.1
			42.63	13.27		6.1	CCI-1996
		1703.1.14	42.67	13.17	6.7		NT4.1.1
			42.68	13.08		6.6	CCI-1996
50	Central Apennines	1792.10.06	42.31	13.59	6.2		NT4.1.1
			42.30	13.58		5.6	CCI-1996
51*	Central Apennines	1461.11.26	42.32	13.53	6.7		NT4.1.1
		11.27	42.30	13.55		6.1	CCI-1996
52	Central Apennines	1298.12.01	42.50	12.88	6.4		NT4.1.1
			42.55	12.83		5.1	CCI-1996
58	Central Apennines	1349.9.0	42.27	13.13	6.4		NT4.1.1
		9.09	42.27	13.10		5.6	CCI-1996
59*	Central Apennines	1915.1.13	42.03	13.49	7.0		NT4.1.1
			41.98	13.62		6.9	CCI-1996

Table 1. Continued...

61*	Central Apennines	1706.11.03 1933.9.26	42.00 42.10 42.10 42.05	14.18 14.05 14.10 14.18	6.4 6.2 	6.8 6.1	NT4.1.1 CCI-1996 NT4.1.1 CCI-1996
69	Gargano Region	1223 1646.5.31	41.84 41.85 41.83 41.87	16.04 16.03 16.00 15.92	6.2 6.4 	5.6 5.6	NT4.1.1 CCI-1996 NT4.1.1 CCI-1996
70*	Apulian Region	1627.7.30	41.73 41.77	15.27 15.32	7.0 	6.1	NT4.1.1 CCI-1996
73*	Central Apennines	1688.6.05 1805.7.26	41.32 41.33 41.50 41.53	14.57 14.67 14.53 14.52	7.3 6.7 	6.1 6.5	NT4.1.1 CCI-1996 NT4.1.1 CCI-1996
74*	Central Apennines	1349.9.0 9.09 1654.7.23	41.53 41.53 41.64 41.65	13.87 14.05 13.71 13.70	6.7 6.4 	6.1 5.6	NT4.1.1 CCI-1996 NT4.1.1 CCI-1996
84*	Southern Apennines	1456.12.05 1702.3.14 1732.11.29 1962.8.21	41.15 41.27 41.12 41.15 41.08 41.07 41.17 41.15	14.87 14.77 14.95 14.97 15.12 14.97 14.97 15.00	6.7 6.4 6.4 6.2 	6.6 6.1 6.1 6.5	NT4.1.1 CCI-1996 NT4.1.1 CCI-1996 NT4.1.1 CCI-1996 NT4.1.1 CCI-1996
85*	Southern Apennines	1361.7.07 1851.8.14 1930.7.23	41.20 41.23 40.95 40.97 41.05 41.03	15.60 15.45 15.65 15.67 15.30 15.35	6.4 6.4 6.7 	5.6 6.8 7.0	NT4.1.1 CCI-1996 NT4.1.1 CCI-1996 NT4.1.1 CCI-1996
86	Apulia Region	1731.3.20	41.32 41.33	15.80 15.82	6.2 	5.6	NT4.1.1 CCI-1996
90*	Southern Apennines	1694.9.08 1853.4.09 1980.11.23	40.90 40.88 40.85 40.78 40.80 40.85	15.43 15.30 15.25 15.22 15.27 15.28	7.0 6.2 6.9 	6.1 5.6 6.7	NT4.1.1 CCI-1996 NT4.1.1 CCI-1996 NT4.1.1 CCI-1996
92*	Iscoa Island	1883.7.28	40.75 40.75	13.89 13.88	6.2 	6.3	NT4.1.1 CCI-1996
95*	Southern Apennines	1561.8.19 1857.12.16	40.54 40.50 40.35 40.37	15.49 15.55 15.83 15.83	6.4 7.0 	5.6 7.0	NT4.1.1 CCI-1996 NT4.1.1 CCI-1996
106	Calabria	1836.4.25	39.57 39.57	16.70 16.73	6.4 	5.6	NT4.1.1 CCI-1996
109*	Calabria	1184.0.0 5.24 1854.2.12 1870.10.04	39.42 39.43 39.27 39.25 39.25 39.22	16.20 16.25 16.27 16.30 16.33 16.33	6.4 6.4 6.4 	5.6 6.8 6.1	NT4.1.1 CCI-1996 NT4.1.1 CCI-1996 NT4.1.1 CCI-1996
112	Calabria	1638.3.27	39.08 39.08	16.28 16.28	7.3 	6.6	NT4.1.1 CCI-1996
113	Calabria	1832.3.08	39.05 39.05	16.92 16.95	6.4 	5.6	NT4.1.1 CCI-1996
117*	Calabria	1626.3.27 4.04 1659.11.05 1791.10.13 1783.2.07	38.82 38.82 38.70 38.68 38.66 38.60 38.58 38.57	16.42 16.42 16.33 16.27 16.25 16.30 16.22 16.18	6.2 6.4 6.2 7.0 	5.1 6.1 5.6 6.2	NT4.1.1 CCI-1996 NT4.1.1 CCI-1996 NT4.1.1 CCI-1996 NT4.1.1 CCI-1996
118*	Calabria	1905.9.08	38.75 38.76	16.03 16.05	7.5 	6.5	NT4.1.1 CCI-1996

Table 1. Continued...

123*	Sicily	1968.1.15	37.75 37.77	12.97 12.98	6.4	7.1	NT4.1.1 CCI-1996
127	Sicily	1978.4.15	38.15 38.27	14.98 15.10	6.1	5.8	NT4.1.1 CCI-1996
128*	Calabria	1908.12.28	38.13 38.18	15.67 15.68	7.3	7.0	NT4.1.1 CCI-1996
129*	Calabria	1783.2.05	38.27 38.30	15.92 15.97	7.3	7.1	NT4.1.1 CCI-1996
130	Calabria	1928.3.07	38.63 38.60	15.98 16.78	5.9	6.0	NT4.1.1 CCI-1996
136	Sicily	1818.2.20 1911.10.15	37.62 37.60 37.70 37.70	15.10 15.12 15.17 15.15	6.2 5.1	5.6 6.3	NT4.1.1 CCI-1996 NT4.1.1 CCI-1996
144*	Sicily	1169.2.04 1693.1.11	37.33 37.32 37.33 37.42	15.20 15.03 15.10 15.05	7.3 7.3	6.1 7.5	NT4.1.1 CCI-1996 NT4.1.1 CCI-1996

Note:

** For historical event M_s is derived from M_1 by means of the relation (53): $M_s = 0.56(+/-0.017)\ I_0 + 0.94\ (+/-0.13)$.
Nodes hosting events with $M \geq 6.0$ in both catalogues are marked by (*).

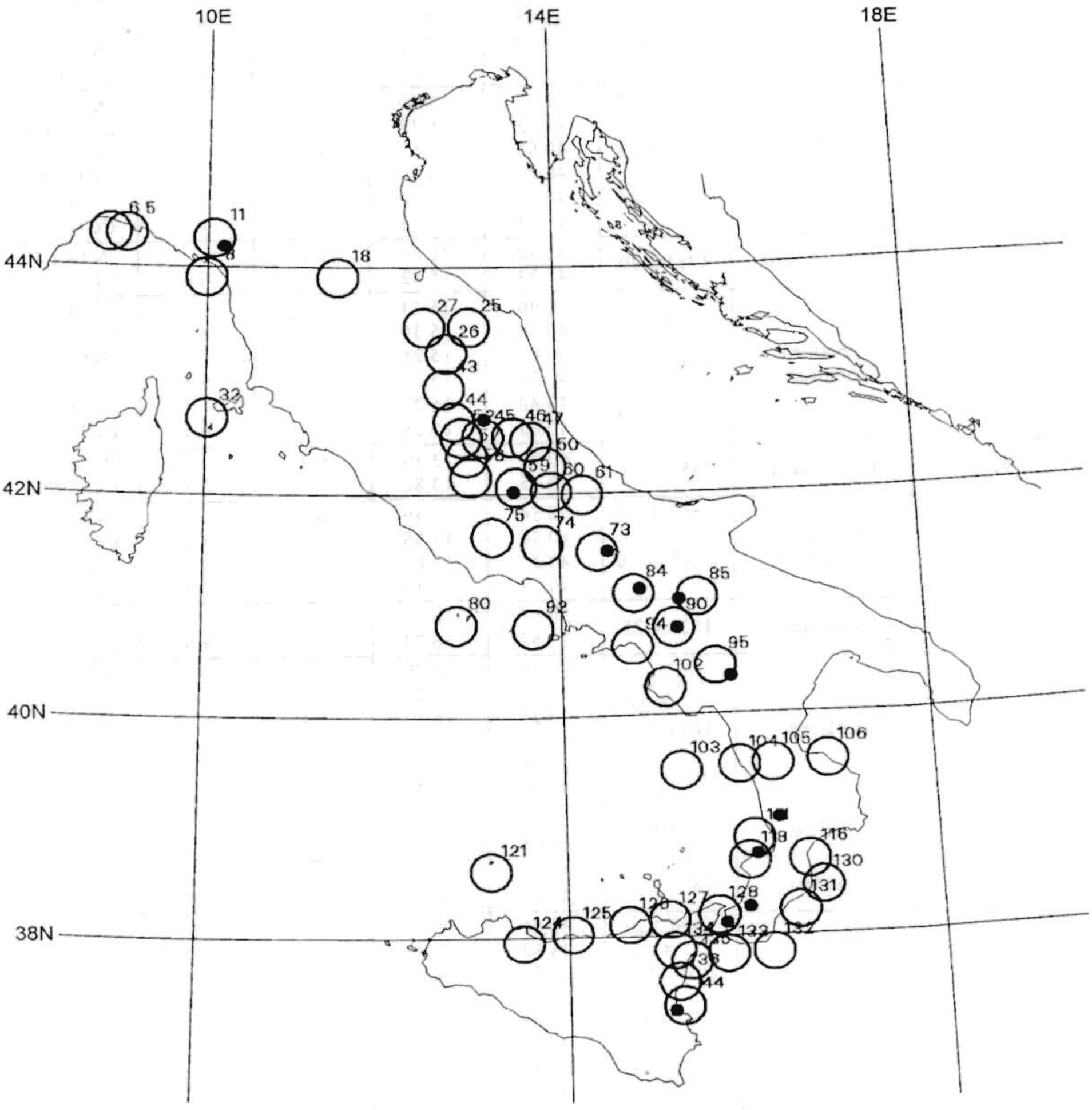

Figure 3. Result of the identification of the nodes prone to earthquakes with $M \geq 6.5$. Dots are the epicenters with $M \geq 6.5$ listed in Table (1). Circles are the nodes recognized to be prone to earthquakes with $M \geq 6.5$. Numbering of nodes as in Table (4).

quakes potential ($M \geq 6.5$) are identified by the criteria of high seismicity derived by Kossobokov [24] from pattern recognition in the Pamirs-Tien Shan region.

5.1. Recognition of Nodes Prone to Earthquakes with $M \geq 6.0$

5.1.1. Parameters of the Nodes Used for the Recognition and Their Discretization

In order apply recognition algorithm (see section 2.2) each node is described by the set of parameters listed in Table (2). The parameters are very simple and are based on widely available morphometric, gravity and morphostructural data. They have been tested in previous investigations by pattern recognition of earthquake-prone areas and have been found sufficiently informative to identify the seismogenic nodes [3, 9, 15, 16, 17, 18, 19, 20, 21].

The parameters, see Table (2) referring to the topographic altitudes and to the area of soft sediments characterize indirectly the intensity of recent tectonic movements, and those referring to density of lineaments and gravity indicate the degree of the crust fragmentation

Table 2. Parameters, used for pattern recognition, and thresholds of their discretization.

Parameters	Thresholds of Discretization
A) Topographic parameters	
Maximum topographic altitude, *m* (*Hmax*)	1500
Minimum topographic altitude, *m* (*Hmin*)	- 230 80
Relief energy, *m* (ΔH) (*Hmax-Hmin*)	1500 2000
Distance between the points Hmax and Hmin, *km* (*L*)	35
Slope, ($\Delta H/L$)	0.040 0.065
B) Geological parameters	
The portion of soft (Quaternary) sediments, %, (*Q*)	1 5
C) Gravity parameters	
Maximum value of Bouguer anomaly, *mGal*, (*Bmax*)	10 47
Minimum value of Bouguer anomaly, *mGal*, (*Bmin*)	-46 7
Difference between *Bmax* and *Bmin*, *mGal*, (ΔB)	44 66
D) Parameters from the morphostructural map	
The highest rank of lineament in a node, (*HR*)	1
Number of lineaements forming a node, (*NL*)	2
Distance to the nearest 1st rank lineament, *km*, (*D1*)	0 50
Distance to the nearest 2nd rank lineament, *km*, (*D2*)	0 50
Distance to the nearest node, *km*, (*Dn*)	23 30
E) Morphological parameter (Mor)	
This parameter is equal to one of the following six values in accordance with the morphology within each node: 1- mountain and plain (*m/p*) 2- mountain and piedmont (*m/pd*) 3- mountain and mountain (*m/m*) 4. piedmont and plain (*pd/p*) 5. piedmont only (*pd*) 6. plain only	2 4

and dislocation.

The values of the parameters have been measured from topographic, geological, gravity and morphostructural maps within the areas of radius of $25km$ around the points of intersection of the lineaments.

The discretization has been done with the *a priori* division of the nodes into sets D_0 and N_0. The histogram for each parameter has been constructed and the thresholds for the discretization have been defined, see Table (2) so that the nodes are divided into two or three groups. Each group includes approximately the same number of nodes. The discretization of the morphological parameter *Mor*, see Table (2) has been made with two thresholds: 2 and 4. After the coding this parameter is converted into three binary components: 100,010, and 001, if its value in Table (2) is (1 or 2), (3 or 4) and (5 or 6), respectively.

5.1.2. Recognition of the Nodes Capable of Earthquakes with $M \geq 6.0$

5.1.2.1. Selection of the Training Set

In total, 146 nodes have been delineated by *MZ*. Within 43 nodes earthquakes with $M \geq 6.0$ already took place according to at least one of the two catalogues used, see Table (1).

At the learning stage (see Section 2.2) all the nodes are *a priori* divided into three sets. To make the results more robust, we include in the set D_0 only the nodes, marked by (*) in Table (1), hosting earthquakes with $M >= 6.0$ in both catalogues. The nodes, where events with $M \geq 6.0$ have not been recorded till present, are assigned to the set N_0. The set X includes 1) the nodes hosting earthquakes with $M >= 6.0$, in at least one of two catalogues used, and 2) the nodes situated in flat areas of low seismicity (Adriatic foreland and Tyrrhenian shelf). The training set for "*CORA*-3" algorithm is formed by D_0 and N_0 sets. The nodes of the set X are not used for the selection of the characteristic traits of D and N nodes.

The results of the learning stage are shown in Table (3). The characteristic traits of D and N nodes have been obtained by "*CORA*-3" with the following values of the thresholds: $k_1 = 4$, $\bar{k}_1 = 2, k_2 = 13$, $\bar{k}_2 = 0$. The classification obtained with these parameters of the "*CORA*-3" algorithm is the most stable of the analyzed variants of classification.

The obtained characteristic traits, represented in Table (3), are defined by six parameters of the nodes: relief energy (ΔH), gradient of topography ($\Delta H / L$), minimal value of Bouguer anomaly (*Bmin*), highest rank of lineament (*HR*), distance to the nearest second rank lineament (D_2), and morphology (*Mor*). The relatively small values of the thresholds k_1 and k_2 as compared with the numbers of objects in D_0 and N_0 sets are justified by the preliminary analysis that allowed us to reduce the whole list of parameters describing the nodes to these six parameters only.

The classification has been made with $\Delta = 0$ (see Section 2.2), i.e. a node is assigned to the D set, if the difference between the number of D - and N - traits, which a given node possess, is greater or equal to 0 (decision rule 1).

81 (55%) out of the 146 nodes considered are recognized to be capable of $M \geq 6.0$ earthquakes. They are marked by (+) in Table (4) and shown by circles with identification numbers in Figure (2).

It follows from Table (4) that the decision rule 1 can be simplified as follows: a node is assigned to the D set if it does not possess N -traits at all, if a node possesses at least one N -trait of those five listed in Table (3) then it is assigned to the N set. This confirms with the zero value of the threshold $\bar{k}_2$ because, as follows from the definition

Table 3. Characteristic features of *D* and *N* nodes.

#	ΔH	ΔH/L	Bmin	HR	D2	*Mor*
Characteristic traits of class **D** (**D**-traits)						
1	$\leq 2000m$	>0.065				*m/m* or *pd/p*
2	$\leq 1500m$	> 0.040				*m/m* or *pd/p*
3	$\leq 2000m$		> 7mGal			*m/m* or *pd/p*
Characteristic traits of class **N** (**N**-trait)						
1		>0.040				not (*m/m* or *pd/p*)
2	$\leq 1500m$	≤0.040	≤ 7mGal			
3			≤7mGal			not (*m/m* or *pd/p*)
4				≤ 1		not (*m/m* or *pd/p*)
5					>50*km*	not (*m/m* or *pd/p*)

of the characteristic traits (section 2.2) if $\bar{k}_2 = 0$ than *N*-traits should not be found in the nodes of the set D_0.

The stability of the classification obtained has been tested in the series of control experiments, which were implemented in other studies on pattern recognition of earthquake-prone areas [*e.g.*, 3, 16, 17, 18, 19, 20, 21]. The results of these experiments are given in the Appendix.

5.1.3. Identification of the Nodes Where Earthquakes with $M \geq 6.5$ May be Nucleated

In order to identify the nodes where earthquakes with $M \geq 6.5$ may occur, we use the morphostructural criteria determined by pattern recognition of high seismicity nodes in the Pamir-Tien Shan region [24], where according to these criteria, the nodes prone to earthquakes with $M \geq 6.5$ possess at least two of the following four features:

1. The relief energy is greater than $2500m$;
2. The combination of the morphology within a node is *m*/*m*, see Table (2);
3. The highest rank of one of the lineaments forming a node is either one or two;
4. The number of lineaments forming a node is greater than two.

Previous studies proved the applicability of these criteria to the identification of high potential seismic nodes. The nodes of the Greater Caucasus [19], Carpatho-Balkan mountain belt [25] and Kopet Dagh region [26] have been classified, using these criteria, to define where earthquakes with $M \geq 6.5$ may occur.

In these regions, all the nodes hosting the known $M \geq 6.5$ events have been defined prone to earthquakes with such magnitudes. The 1991 Racha earthquake with $M = 6.8$ proves the validity of the results for the Greater Caucasus: the event occurred at the node previously identified by Gvishiani et al [19] prone to $M \geq 6.5$ events.

The tested criteria have not a direct and intimate connection with the geodynamical environments of the region where they have been defined, and their applicability to other seismic regions has been discussed by Gorshkov et al [25], therefore the criteria can be used for the identification of high seismicity nodes in the studied region.

The topography on the Pamirs-Tien Shan region is much higher as compared to the one in the region considered, therefore the parameter "relief energy" has to be normalized accordingly to the topography elevation in the studied region. Following the normalization procedure described by Gorshkov et al [25] for the Carpatho-Balkan mountain belt, the threshold for this parameter, in the region considered, has been found to be greater than $1500m$. In order to guarantee some robustness to our results, we decided that each node prone to $M \geq 6.5$ events must possess three out of the four features listed at the beginning of this Section.

As a result, 53 (36%) out of the 146 nodes have been classified to be prone to earthquakes with $M \geq 6.5$. They are indicated by (•) in Table (4) and shown by circles with identification numbers in Figure (3).

The result of the classification of the nodes hosting earthquakes with $M \geq 6.5$ in both catalogues is given in Table (5).

In Calabria, only two nodes (118 and 128) hosting earthquakes with $M \geq 6.5$, in both catalogues, out of four are recognized, while in the Apennines and Sicily all of them are recognized.

6. Discussion and Conclusion

The nodes have been delineated by morphostructural zonation around the Adria margin in peninsular Italy and Sicily. The nodes of high seismic potential and their characteristic features have been defined by pattern recognition. Many large Italian cities are situated within the seismogenic nodes, see Table (6).

Seismogenic nodes (*D*) differ form non-seismogenic ones (*N*) mainly in the morphology within the node, see Table (3). According to the characteristic traits, *D* nodes are mostly located either within mountain chain (morphology *m*/*m*) or at the boundaries between piedmonts and plains (morphology *pd*/*p*), while *N* nodes are characterized by any other morphology listed in Table (2), except *m*/*m* and *pd*/*p*. In addition, *N* nodes should be positioned relatively far from the second-rank lineaments ($D2 > 50km$) see Table (3). In Figure (2) one can see that *D* nodes are basically related with first- and second-rank lineaments, while the overwhelming majority of *N* nodes is formed by third-rank lineaments.

The classification of the nodes for both magnitude thresholds considered do not contradict the recorded strong earthquakes. All earthquakes assigned to $M \geq 6.0$ in both catalogues are located at the nodes recognized prone to $M \geq 6.0$. The same is true for most of the events with $M \geq 6.0$ at least in one of the catalogues, except those situated at the nodes 17, 20, 21, 28, 38, and 39, see Table (1). But in close vicinity of these nodes, except node 21, there are other *D* nodes, see Figure (2) and corresponding earthquakes in fact can be connected with them. Thirteen out of the fifteen nodes hosting $M \geq 6.5$ events in both catalogues are properly classified, the failures being nodes 112 and 129 in Calabria.

The classifications for both magnitude thresholds are in a good agreement: nodes prone to $M \geq 6.5$ earthquakes are simultaneously capable of $M \geq 6.0$ events, except node 47.

It total, 81 nodes have been recognized to be prone to earthquakes with $M \geq 6.0$, see Table (4). At 44 of them strong events have not been recorded till present, however some of them are associated with paleoseismicity. In particular, (1) near to nodes 99, related to the Pollino fault, and 105, related to the Palinuro fault [30], which is

Table 4. Voting and classification of the nodes.

Node #	Number of traits ($M \geq 6.0$) possessed by nodes: D-traits	N-traits
Nodes of set D_0		
11 + •	0	
26 + •	2	0
27 + •	0	0
43 + •	2	0
45 + •	0	0
51 +	0	0
59 + •	1	0
61 + •	0	0
70 +	1	0
73 + •	1	0
74 + •	0	0
84 + •	0	0
85 + •	1	0
90 + •	1	0
92 + •	2	0
95 + •	0	0
109 +	0	0
112 +	1	0
117 +	1	0
118 + •	0	0
123 +	0	0
128 + •	0	0
129 +	0	0
144 + •	0	0
Nodes of set N_0		
1	0	1
2	0	1
4	0	3
5 + •	0	0
6 + •	0	0
8 + •	0	0
10	0	2
12	0	3
13	0	3
19	0	2
29	0	2
30	0	1
33	0	1
34	0	1
35	0	2
36 +	0	0
37	0	2
40	0	4
42	0	3
44 + •	0	0
46 + •	0	0
47 •	0	3
49	0	3
53	0	1
56	0	2
57 + •	0	0
60 + •	0	0
62	0	1
72	0	1
75 + •	0	0
76	0	2
77	0	1
81	0	1
83	0	2
89	0	4
91	0	3
94 + •	0	0
96	0	4
98	0	4
99 +	0	0
101 +	0	0
102 + •	2	0
104 + •	0	0
105 + •	0	0
107	0	4
108 +	0	0
110	0	1
111 + •	0	0
114	0	4
115	0	3
116 + •	0	0
124 + •	0	0
125 + •	0	0
126 + •	0	0
131 + •	0	0
132 + •	0	0
133 + •	0	0
134 + •	0	0
135 + •	0	0
137	0	2
138 +	0	0
139	0	2
140	0	3
143	0	1
145 +	1	0
146	0	2
Nodes of set X		
3	0	2
7	0	2
9	0	3
14	0	2
15	0	2
16	0	2
17	0	1
18 + •	0	0
20	0	1
21	0	1
22	0	2
23	0	2
24	0	2
25 + •	0	0
28	0	1
31	0	3
32 + •	1	0
38	0	1
39	0	3
41 +	0	0
48	0	1
50 + •	0	0
52 + •	1	0
54	0	2
55	0	1
58 + •	0	0
63 +	0	0
64	0	1
65 +	0	0
66 +	0	0
67 +	0	0
68 +	0	0
69 +	1	0
71	0	1
78	0	2
79	0	3
80 + •	0	0
82 +	0	0
86 +	1	0
87 +	0	0
88 +	0	0
93 +	1	0
97	0	1
100	0	1
103 + •	0	0
106 + •	0	0
113 +	0	0
119 +	0	0
120 +	0	0
121 + •	0	0
122	0	2
127 + •	0	0
130 + •	0	0
136 + •	0	0
141	0	1
142 +	0	0

Note:

+ - Nodes recognized to be potential for $M \geq 6.0$.

• - Nodes recognized to be potential for $M \geq 6.5$.

Table 5. Classification of the nodes with earthquakes with M ≥ 6.5 in both catalogues.

Region	Number of Events with M ≥ 6.5 in Both Catalogues Used	Number of the Node with Events of M ≥6.5	Result of Classification for M ≥ 6.5
Apennines	9	11	Recognized
		25	Recognized
		45	Recognized
		59	Recognized
		73	Recognized
		84	Recognized
		85	Recognized
		90	Recognized
		95	Recognized
Calabria	4	*112*	*Not Recognized*
		118	Recognized
		128	Recognized
		129	*Not Recognized*
Sicily	1	144	Recognized

Table 6. Large cities situated within seismogenic nodes.

City	Node Number	Estimated Magnitude
500,000-1,000,000 Inhabitants		
Genova	6	≥ 6.5
Palermo	124	≥6.5
100,000-500,000 Inhabitants		
Ancona	25	≥ 6.5
Catania	136	≥ 6.5
Cosenza	109	≥ 6.0
Firenze	18	≥6.5
Foggia	70	≥ 6.0
La Spezia	8	≥ 6.5
Messina	128	≥ 6.5
Perugia	36	≥6.0
Pescara	48	≥ 6.0
Reggio di Calabria	128	≥6.5
Salerno	94	≥ 6.5
Siracus	145	≥ 6.0
Taranto	97	≥ 6.0
Terni	52	≥ 6.5

Note: Roma and Napoli are situated at the distance of 30-50*km* from the nodes 58 (M ≥ 6.5) and 92 (M ≥ 6.5), respecitvely.

referred also as Sangineto line by Ghisetti & Vezzani [29], paleoseismological evidences of high-intensity events have been determined by Michetti et al [51], (2) evidences of Holocene activity of the neighboring Castrovillari fault are reported by Cinti et al [52], and (3) near to node 44, close to the Rieti basin, paleoseismological evidences have been identified by Michetti et al [40]. Most of the nodes of high seismic potential fall into the seismogenic zones outlined by Meletti at al [8], with the exclusion of the nodes located in the Apulian region and within the Adriatic and Tyrrhenian shelf.

The space distribution of seismogenic nodes, mainly for the ones capable of events with $M \geq 6.5$, mimics quite well the belt marking the transition from normal to soft/thin lid delineated by Calcagnile & Panza [37], and it is relevant for seismic hazard assessment. In fact, according to the recorded seismicity (see e.g. the seismicity map by Meletti et al [8]), some seismogenic nodes are located in low seismicity or aseismic areas, like node 86 in the Apulian region, and nodes 32, 80, 93 at the boundary between the Tyrrhenian basin and the shelf zone.

In the Northern Apennines, *D* nodes are clustered in their western part. In the central Apennines, the seismogenic nodes are mainly situated inside the high-topography belt and along the contact of mountains with low or flat topography areas; most of them are prone both to $M \geq 6.0$ and $M \geq 6.5$ events. In the Southern Apennines, most of the nodes are identified to have high seismic potential. In Calabria, the nodes having the higher potential ($M \geq 6.5$) are associated with the first- and second-rank lineaments surrounding the mountain country. In the inner part of Calabria, the seismogenic nodes are identified prone to $M \geq 6.0$ quakes but non-prone to $M \geq 6.5$ events. In Sicily, the seismogenic nodes form two linear zones along the northern and eastern coastlines. In the Gargano region, the seismogenic nodes surround the promontory and are prone to events with $M \geq 6.0$, but are not capable of larger earthquakes ($M \geq 6.5$). The same is true for nodes 86, 88, 123, 142, and 145 situated within the Adria-Africa foreland. The nodes in the Adriatic Sea (65, 66, 67, 68, and 87) at the border of the study area are classified as *D* (for $M \geq 6.0$). There are no epicenters of earthquake with $M \geq 6.0$ in the vicinity of these nodes, and even if earthquakes with $M \geq 5.0$ have been recorded nearby nodes 66, 65, and 67, we are not sure that the nodes within the Adriatic Sea are really prone to $M \geq 6.0$ earthquakes, and their recognition may be affected by some kind of border effect. Seismic potential of these nodes will be re-evaluated in separate study of the region, which will include other nodes within the Adriatic Sea.

We have compared the nodes recognized in this study to be potential for $M \geq 6.0$ with those determined by Caputo et al [3]. Obviously we compare the spatial distribution of the seismogenic nodes only within peninsular Italy and Sicily. Due to the different scale of the morphostructural zonation performed in the two studies, the total number of nodes and their geographical position are not the same. Our decision rule for the classification of nodes into *D* and *N* has been formulated in a simple way on the basis of only the five *N*-traits given in Table (3) (see section 5.1.2) while 7 *D* -traits and 7 N-traits are used in the decision rule adopted by Caputo et al [3]. Sufficiently good agreement can be seen in the Central Apennines, central Calabria and northern Sicily, while there is some difference in the Northern Apennines and in the inner part of Sicily. In the Northern Apennines the seismogenic nodes determined by Caputo et al [3] form a relatively large zone, while in our study only two nodes 11 and 18 have been classified as *D*. In Sicily, there is agreement in the northern part of the island but, unlike us, Caputo et al [3] recognized some nodes as *D* in the inner part of Sicily.

Some nodes are recognized as *D* by our study in the areas where the nodes have not been delineated by Caputo et al [3] due to the smaller scale of the morphostructural zonation. They are nodes 25, 26, 36, 41, and 43 in the transition zone between the Northern and Central Apennineses, nodes 88, 94, 95 and 102 in the Southern Apennines, and the nodes located along the eastern offshore of Calabria. The main difference between the results concerns the classification of the nodes located within the Tyrrhenian and Adriatic seas. Many of these nodes are recognized by our study to be potential for the occurrence of events with $M \geq 6.0$, while all the nodes within the marine shelf have been classified as *N* by Caputo et al [3].

We consider the results illustrated in this paper as a first step in the study of earthquake-prone areas around the Adria margin. This step will be a major interdisciplinary effort and attempt to explain how the structure and the dynamics of the lithosphere in the region brings into existence the seismogenic nodes at the sites determined in this work.

7. Acknowledgments

This research has been partly done at the Abdus Salam International Center for Theoretical Physics (Trieste, Italy) and supported by a subcontract with Cornell University, Geological Sciences, under *EAR*-9804859 from the U.S. National Science Foundation and administered by the U.S. Civilian Research & Development Foundation for the Independent States of the Former Soviet Union (*CRDF*) and by the International Science and Technology Center (Moscow, Project #1293). Support from *MURST* (40% and 60% funds) has been essential. A. Gorshkov was supported by *CNR-NATO* Guest Fellowships Programme 1998 (Pos. 220.323). This is a contribution to *UNESCO-IUGS-IGCP* Project 414. The authors are grateful to Profs I. Rotwain, C. Doglioni, and L. Serva for very useful discussions and suggestions.

References

1. Lort, J.M. (1971). "The tectonics of the Eastern Mediterranean", *Rev. Geophysics*, **9**, 189-216.

2. Anderson, H.J. and Jackson, J. (1987). "Active Tectonics of the Adriatic Region", *Geophys. J. R. Astron. Soc.*, **91**, 937-938.

3. Caputo, M., Keilis-Borok, V., Oficerova, E., Ranzman, E., Rotwain, I., and Solovieff, A. (1980). "Pattern Recognition of Earthquake-Prone Areas in Italy", *Phys. Earth Planet. Inter.*, **21**, 305-320.

4. Alessio, G., Esposito, E., Gorini, A., Luongo, G., and Porfido, S. (1993). "Identification of Seismogenic Areas in the Southern Apennines, Italy", *Annali di Geofisica*, **36**(1), 227-235.

5. Boschi, E., Gasperini, P., and Mulargia, F. (1995). "Forecasting where Larger Crustal Earthquakes are Likely to Occur in Italy in the Near Future", *Bull. Seismol. Soc. Amer.*, **85** (5), 1475-1482.

6. Molchan, G.M., Kronrod, T.L., and Panza, G.F. (1997). "Multiscale Seismicity Model for Seismic Risk", *Bull. Seismol. Soc. Am.* **87**(5), 1220-1229.

7. Panza, G.F., Vaccari, F., and Cazzaro, R. (1999). "Deterministic Seismic Hazard Assessment", *F. Wenzel et al (eds.), Vrancea Earthquakes: Tectonics, Hazard and Risk Mitigation*, 269-286.

8. Meletti, C., Patacca, E., and Scandone, P. (2000). "Construction of a Seismotectonic Model: The Case of Italy", *PAGEOPH*, **157**, 11-35.

9. Gelfand, I., Guberman, Sh., Izvekova, M., Keilis-Borok, V., and Rantsman, E. (1972), "Criteria of High Seismicity, Determined by Pattern Recognition", *Tectonophysics*, **13**, 415-422.

10. Gvishiani, A. and Soloviev, A. (1980). "On the Concentration of the Major Earthquakes Around the Intersections of Morphostructural Lineaments in South America", In V.I. Keilis-Borok and A.L. Levshuin (eds), Methods and Algorithms for Interpretation of Seismological Data. Nauka, Moscow, 46-50 (Computational Seismology, Iss.13, in Russian).

11. McKenzie, D.P. and Morgan, W.J. (1969). "The Evolution of Triple Junctions", *Nature*, **224**, 125-133.

12. Gabrielov, A., Keilis-Borok, V., and Jackson, D. (1996). "Geometric Incompatibility in a Fault System", *Proc. Natl. Acad. Sci. USA*, **93**, 3838-3842.

13. Alekseevskaya, M.A., Gabrielov, A.M., Gvishiani, A.D., Gelfand, I.M., and Ranzman, E.Ya. (1977). "Formal Morphostructural Zoning of Mountain Territories", *J. Geophys*, **43**, 227-233.

14. Rantsman, E.Ya. (1979). "Morphostructure of Mountain Regions and Sites of Earthquakes", Nauka, Moscow (In Russian).

15. Bhatia, S.C., Chetty, T.R.K., Filimonov, M., Gorshkov, A., Rantsman E., and Rao, M.N. (1992). "Identification of Potential Areas for the Occurrence of Strong Earthquakes in Himalayan arc Region", *Proc. Indian Acad. Sci. (Earth Planet Sci.)*, **101**(4), 369-385.

16. Cisternas, A., Godefroy, P., Gvishiani, A., Gorshkov, A., Kossobokov, V., Lambert, M., Rantsman, E., Sallantin, J., Saldano, H., Soloviev, A., and Weber, C. (1985). "A Dual Approach to Recognition of Earthquake Prone Areas in the Western Alps", *Annale Geophysicae*, **3**(2), 249-270.

17. Gelfand, I., Guberman, Sh., Keilis-Borok V., Knopoff, L., Press, F., Rantsman, E., Rotwain, I., and Sadovsky, A. (1976). "Pattern Recognition Applied to Earthquake Epicentres in California", *Phys. Earth Planet. Inter.*, **11**, 227-283.

18. Gorshkov, A., Zhidkov, M., Rantsman, E., and Tumarkin, A. (1991). "Morphostructures of the Lesser Caucaus and Sites of Earthquakes, M 5.5", *Izvestyia USSR Ac. Sci., Physics of the Earth.*, **6**, 30-38 (in Russian).

19. Gvishiani, A., Gorshkov, A., Kossobokov, V., and Rantsman, E. (1986). "Morphostructures and Earthquake-prone areas in the Great Caucasus", *Izvestyia USSR Ac. Sci., Physics of the Earth.*, **9**, 15-23 (in Russian).

20. Gvishiani, A., Gorshkov, A., Kossobokov, V., Cisternas, A., Philip, H., and Weber, C. (1987). "Identification of Seismically Dangerous Zones in the Pyrenees", *Annales Geophysicae*, **5B**(6), 681-690.

21. Gvishiani, A., Gorshkov, A., Rantsman, E., Cisternas, A., and Soloviev, A. (1988). "Identification of Earth quake-Prone-Areas in the Regions of Moderate Seismicity", Nauka, Moscow, (in Russian).

22. Guberman, Sh.A. and Rotwain, I.M. (1986). "Checking of the Predictions of Earthquake Prone Areas (1974-1984)", *Izvestyia USSR Ac. Sci., Physics of the Earth.*, **12**, 72-84 (in Russian).

23. Gorshkov, A., Kossobokov, V., Rantsman, E., and Soloviev, A. (2001). "Recognition of Earthquake Prone Areas: Validity of the Results Obtained from 1972 to 2000", In V.I., Keilis-Borok and G.M. Molchan (eds), Computational Seismology, Iss.32, 48-57, (in Russian).

24. Kossobokov, V.G. (1983). "Recognition of the Sites of Strong Earthquakes by Hamming's Method in East Central Asia and Anatolia", In V.I. Keilis-Borok and A.L. Levshuin (eds), Computational Seismology, Iss.14. Allerton Press, Inc., New York., 78-82.

25. Gorshkov, A., Kuznetsov, I., Panza, G., and Soloviev, A. (2000a). "Identification of Future Earthquake Sources in the Carpatho-Balkan Orogenic Belt Using Morphostructural criteria", *PAGEOPH*, **157**, 79-95.

26. Gorshkov, A., Piotrovskaya, E., and Rantsman, E. (2002). "Identification of Earthquake Prone Areas in the Kopet Dagh", In V.I. Keilis-Borok and G.M. Molchan (eds), Computational Seismology, Iss.33 (In Press, In Russian).

27. Ruthen, M.G. (1969). "The Geology of Western Europe", Elsilver P.C. Amsterdam.

28. AA.VV. (1983). Structural Model of Italy, Scale 1:500,000. CNR, Rome, Italy

29. Ghisetti, F. and Vezzani, L. (1981). "Contribution of Structural Analysis to Understanding the Geodynamic Evolution of the Calabrian Arc (Southern Italy)", *Journal of Struct. Geology*, **3**(4), 371-381.

30. Mantovani, E., Albarello, D., Babbuccci, D., and Tamburelli, C. (1997). "Recent/Present Tectonic Processes in the Italian Region and Their Relation with Seismic and Volcanic Activity", *Annales Tectonicae*, **11**(1-2), 27-57.

31. International Tectonic Map of Europe and Adjacent Areas (1981). Second Edition. Moscow: Acad. Sci. USSR-UNESCO.

32. Carmignani, L., Decandia, A., Fantozzi, L., Lazzarotto, A., Liotta, D., and Meccheri, M. (1994). "Tertiary Extensional Tectonics in Tuscany (Northern Apennines, Italy)", *Tectonophysics*, **238**, 295-315.

33. Philip, H. (1983). "Carte de la Tectonique Actuelle et Recente du Domaine Mediterraneen et de la Chaine Alpine", Publication de l'Institut National d' Astronomie et Geophysique I.N.A.G. C.N.R.S. Paris.

34. Anelli, L., Capelli, V., and Torre, P. (1998). "Interpretation of Northern-Apennine Magnetic and Gravity Data in Relation to the Profile CROP-3", *Mem. Soc. Geol.It*, **52**, 413-425.

35. Scarascia, S., Cassinis, R., and Federici, F. (1998). "Gravity Modeling of Deep Structures in the Northern-Central Apennines", *Mem. Soc. Geol. It*, **52**, 231-246.

36. Morelli, C. (1998). "Lithospheric Structure and Geodynamics of the Italian Peninsula Derived from Geophysical Data: a Review". *Mem. Soc. Geol.It.*, **52**, 113-122.

37. Calcagnile, G. and Panza, G.F. (1980). "The Main Characteristics of the Lithosphere-Asthenosphere System in Italy and Surrounding Regions", *PAGEOPH*, **119**, 865-879.

38. Marson, I., Panza, G.F., and Suhadolc, P. (1995). "Crust and Upper Mantle Models Along the Active Tyrrhenian rim", *Terra Nova*, **7**, 348-357.

39. Wise, D.U., Funiciello, R., Parotto, M., and Salvini, F. (1985). "Topographic Lineament Swarms: Clues to their Origin from Domain Analysis of Italy", *Geol. Soc. Bull. Am.*, **96**, 952-967.

40. Michetti, A., Brunamonte, F., Serva, L., and Whitney, R. (1995). "Seismic Hazard Assessment from Paleoseismological Evidence in the Rieti Region, Central Italy", In L. Serva (Ed.), Perspectives in Paleoseismology, Association of Engineering Geologists Special Publication, **6**, 63-82.

41. Galadini, F., Galli, P., Giraudi, C., and Molin, D. (1995). "Il Terremoto del 1915 e la Sismicita Della Piana del Fucino (Italia Centrale)", *Boll. Geol. It.*, **114**, 635-663.

42. Salvini, F. (1993). "Block Tectonics in Thin-Skin Style-Deformed Regions: Examples from Structural Data in Central Apennines", *Annali di Geofisica*, XXXVI, **2**, 97-111.

43. Bousquet, J.C., Grellet, B., and Sauret, B. (1993). "Neotectonic Setting of the Beneveto Area: Comparison with the Epicentral Zone of the Irpina Earthquake", *Annali di Geofisica*, **36**(1), 245-251.

44. Bousquet, J. C. (1973). "La Tectonique Recente de l'Apennin Calabro-Lucanien Dans Son Cadre Geologique et Geophysique", *Geol. Rom.*, **12**, 1-104.

45. Ambrosetti, P., Bosi, C., Carraro, F., Ciaranfi, N., Panizza, M., Papani, G., Vezzani, L., and Zanferrari, A. (1987). Neotectonic Map of Italy, CNR-PFGeodinamica.

46. Moretti, A. and Guerra, I. (1997). "Tettonica dal Messiniano ad Oggi in Calabria: Implicazioni Sulla Geodinamica del Sistema Tirreno-Arco Calabro", *Boll. Soc. Geol. It.*, **116**, 125-142.

47. Riznichenko, Yu.V. (1976). "Source' Dimensions of a Shallow Earthquake and Seismic Moment", In Research on the Physics of Earthquakes, Nauka, Moscow, 9-27 (in Russian).

48. Wells, D.L. and Coppersmith, K.J. (1994). "New Empirical Relationships Among Magnitude, Rupture Length, Rupture Width, and Surface Displacement", *Bull. Seism. Soc. Am.*, **84**, 974-1002.

49. Camassi, R. and Stucchi, M. (1997). "Un Catalogo Parametrico di Terremoti di Area Italiana al di Sopra Della Soglia di Danno", Open Data File, Consiglio Nazionale Delle Ricerche GNDT, NT 4.1.

50. Peresan, A., Costa, G, and Vaccari, F. (1997). "CCI1996: the Current Catalogue of Italy", Internal Report IC/IR/97/9, Miramare-Trieste.

51. Michetti ,A.M., Ferreli, L., Serva, L., and Vittori, E. (1997). "Geological Evidence for Strong Historical Earthquakes in an "Aseismic "Region: the Polino Case (Southern Italy)", *J. Geodynamics*, **24** (1-4), 67-86.

52. Cinti, F. R., Cucci, L., Pantosti, D., D'Addezio, G, and Meghraoui, M. (1997). "A Major Seismogenic Fault, in a Silent Area: The Castrovillari Fault (Southern Apennines, Italy)", *Geophys. J. Int.*, **130**, 595-605.

53. Rebez, A. and Stucchi, M. (1996). "La Determinazione Della Ms a Partire da Dati Macrosismici Per Iterremoti Compresi nei Cataloghi NT", GNDT, Rapporto Interno, Trieste-Milano.

Appendix

Control Experiments

The following control experiments have been performed to test the stability of the result of recognition of the nodes prone to earthquakes with $M \geq 6.0$. The node classification reported in Table 4 will be called the *main variant.*

"Seismic Future" (SF). The experiment is performed using as training, instead of D_0 and N_0, the sets D and N, determined by the main variant, and the following four sets of values for the thresholds:

$$SF(a)\, k_1 = 33,\ \bar{k}_1 = 0, k_2 = 21,\ \bar{k}_2 = 0;$$
$$SF(b)\, k_1 = 20,\ \bar{k}_1 = 1, k_2 = 21,\ \bar{k}_2 = 1;$$
$$SF(c)\, k_1 = 6,\ \bar{k}_1 = 2, k_2 = 15,\ \bar{k}_2 = 2;$$
$$SF(d)\, k_1 = 61,\ \bar{k}_1 = 2, k_2 = 21,\ \bar{k}_2 = 0.$$

$\Delta = 0$ in all cases. In cases (a) and (d) the results of the experiment coincide with the main variant. The classification changes for two nodes (97 and 123) in case (b) and for three nodes (71, 72, and 97) in case (c) as compared to the main variant. Therefore for only 2% of the nodes the classification changes.

"Training X Set" (TX). The experiment is performed using instead of D_0 the nodes of the set X which were recognized as D, and instead of N_0 those which were recognized as N. This experiment has been made with two sets of values for the thresholds:

$$TX(a)\, k_1 = 11,\ \bar{k}_1 = 0, k_2 = 6,\ \bar{k}_2 = 0;$$
$$TX(b)\, k_1 = 5,\ \bar{k}_1 = 1, k_2 = 9,\ \bar{k}_2 = 1.$$

$\Delta = 1$ in the both cases. In case (a) for 8 nodes (26, 34, 43, 70, 81, 85, 110, and 145) and in case (b) for 12 nodes (10, 19, 32, 34, 81, 85, 91, 110, 122, 137, 143, and 145) the classification changes. It is less than 9% of the total number of the nodes.

"Sliding Control" (SC). In this experiment we check whether classification of the nodes belonging to the training set is stable when they are excluded from this set. The nodes are classified on the basis of the training sets $D_0 \setminus \omega^i$ and $N_0 \setminus \omega^{i+n_1}$, $i = 1, 2, ..., max(n_1, n_2)$ where n_1 and n_2 are the numbers of the nodes in the training sets D_0 and N_0, respectively, $D_0 \setminus \omega^i$ and $N_0 \setminus \omega^{i+n_1}$ denote the sets D_0 and N_0 from which the nodes ω^i and ω^{i+n_1} are excluded. The first variant discards the objects $\omega^1 \in D_0$ and $\omega^{1+n_1} \in N_0$, the second variant considers them but discards the objects $\omega^2 \in D_0$ and $\omega^{2+n_1} \in N_0$, and so on. If one of the two sets D_0 or N_0 (with a smaller number of objects) has already all its objects discarded once, we proceed only with the other set. There is a change of classification for four nodes of the set D_0 (27, 85, 95, and 123) and for two nodes of the set N_0 (29 and 37) i.e. for less than 7% of the number of nodes in the whole training set.

"Equivalent Traits" (ET). We call two characteristic traits A_1 and A_2 of class D as equivalent if they are both found in the same nodes of the set D_0. Similarly, characteristic traits A_1 and A_2 of class N are called equivalent, if they are both found in the same nodes of the set N_0. Algorithm "*CORA*-3" includes only one trait from each group of equivalent ones to the final list and the result of the classification depends, generally speaking, on the choice of the traits from the groups of equivalent ones. The experiment evaluates how much the obtained classification is stable with respect to such a choice. For the node ω_i let us denote by u^i_{Dj} the number of its traits belonging to the group of the ones equivalent to the *j-th* trait of class D, and by u^i_{Nj} the number of its traits belonging to the group of the ones equivalent to the *j-th* trait of class N. Let us define on the basis of the numbers u^i_{Dj} and u^i_{Nj} the numbers of "votes" in favor of the classes D and N respectively. They are defined by the formulas

$$u^i_D = \sum_{j=1}^{p_D} \frac{u^i_{Dj}}{p^j_D}, \quad u^i_N = \sum_{j=1}^{p_N} \frac{u^i_{Nj}}{p^j_N}.$$

Here P^j_D and P^j_N are the total numbers of traits equivalent to the j *-th* trait of class D, and N, respectively. The j *-th* trait itself is included in the calculation. In the experiment the set D is formed by the objects, which satisfy the condition $u^i_D - u^i_N \geq \Delta$, and the remaining objects form the set N. The classification obtained with this experiment repeats the main variant.

"Clearance of D_0" (CD). We have formed the set D_0

with the nodes which are the closest to the epicenters of the earthquakes with $M \geq 6.0$ in both catalogues. We can not be absolutely sure that the epicenters are connected with these nodes because possibly there are other nodes in the vicinity of the same epicenters. Table (A1) contains all the nodes in the vicinity of the epicenters with $M \geq 6.0$ in both catalogs. The table shows that 15 nodes (11, 27, 45, 59, 73, 74, 84, 85, 90, 92, 95, 109, 112, 123, and 129) occur

Table A1: Nodes in vicinity of the epicenters with M $\geq$ 6.0 in both catalogues.

Year of the Earthquake	Nodes in the Vicinity of the Epicenters (Ordered Accordingly to Increasing Distance)	
	Distance 25*km*	Distance between 25*km* and 35*km*
1920	11	10, 8
1751	26, 37	38, 43
1781	27	28
1997	43, 41	26, 37
1639	45, 46	52, 42, 44
1703	45	52, 44, 46, 42
1461	51, 47, 59, 46	50
1915	59	51, 60
1706	61, 60	49, 62
1933	61, 60, 49	50
1627	70, 71	63, 72
1688		73, 84, 83
1805	73	
1349	74	
1456	84	
1702	84	
1732		84, 90, 85
1962	84	
1851	85, 86	80
1930	85	90
1694	90, 85	
1980	90	
1883	92	93
1857	95	
1854	109	110, 112
1870	109	112, 110
1638	112	109, 111, 110
1659	117, 116	112, 118
1905	118, 111, 117	
1968	123	
1908	128, 129	133
1783	129	128
1169	144, 137	145, 143, 136
1693	144, 137, 143	145, 136

to be the only within a distance of 25 km from the relevant epicenters. In the experiment we apply "*CORA*-3" algorithm keeping in set the D_0 these 15 nodes only and moving the other nodes from D_0 to X. The classification obtained with the experiment with the parameters given in section 5.1.2 repeats the main variant.

"Clusters" (Cl). In this experiment we apply the algorithm "*CLUSTERS*" [17] instead of "*CORA*-3". "*CLUSTERS*" is the modification of "*CORA*-3" designed for the case when (1) the set D_0 consists of S subsets:

$$D_0 = D_0^{\,1} \cup D_0^{\,2} \cup ..... D_0^{S},$$

and (2) it is known a priori that each subset contains at least one object of class D but some objects of the set D_0 may belong to class N. In the learning step the algorithm "*CLUSTERS*" differs from "*CORA*-3": (1) by definition a subset has a trait if at least one object among those, which belong to this subset, has this trait; (2) the trait A is a characteristic trait of class D if

$$K^S(D_0, A) \geq k_1 \text{ and } K(N_0, A) \geq \bar{k}_1.$$

Here $K^S(D_0, A)$ is the number of subsets which have the trait A. In the algorithm "*CLUSTERS*" the determination of the characteristic traits of class N, the voting and the classification are the same as in "*CORA*-3".

In forming the subsets we have considered two variants. In the first case (*C*l-25) subsets associated with the epicenters consist of nodes located at a distance less or equal to $25km$ from a relevant epicenter. In the second case (*C*l-35) this distance is $35km$, the same distance used by Caputo et al [3] to determine the subsets. In both cases one can see from Table (A1) that, as compared with the training sets used in section 4.1.2, some nodes should be moved from N_0 to D_0. The nodes remaining in the set N_0 are used as a new training set N_0 in the application of the algorithm "*CLUSTERS*". The classification obtained in *C*l-25 with the thresholds $k_1 = 6$, $\bar{k}_1 = 2$, $k_2 = 12$, $\bar{k}_2 = 2$ and $\Delta = -1$ differs from the main variant in 21 nodes (25, 27, 35, 36, 47, 49, 63, 65, 66, 67, 68, 71, 72, 82, 87, 88, 99, 122, 123, 137, 142) i.e. in less than 15% of the total number of nodes. In *C*l-35 classification obtained with the thresholds $k_1 = 8$, $\bar{k}_1 = 1$, $k_2 = 8$, $\bar{k}_2 = 3$ and $\Delta = 0$ changes for 27 nodes (18, 25, 27, 32, 36, 37, 47, 49, 62, 63, 65, 71, 72, 94, 95, 99, 103, 104, 105, 108, 110, 113, 122, 127, 130, 131, 138) i.e. for less than 19% of the total number of nodes.

Following the empirical considerations of Gvishiani et al [21] the general conclusion from the results of these experiments summarized in Table (A2) is that the main variant is reasonably stable.

Table A2: Results of control experiments.

Main variant	SFa	SFb	SFc	SFd	TX-a	TX-b	SC	Et	CD	Cl-25	Cl-35
Nodes of set D_0											
11 +●	+	+	+	+	+	+	+	+	+	+	+
26+●	+	+	+	+		+	+	+	+	+	+
27+●	+	+	+	+	+	+		+	+		
43+●	+	+	+	+		+	+	+	+	+	+
45 +●	+	+	+	+	+	+	+	+	+	+	+
51 +	+	+	+	+	+	+	+	+	+	+	+
59 +●	+	+	+	+	+	+	+	+	+	+	+
61 +●	+	+	+	+	+	+	+	+	+	+	+
70+	+	+	+	+		+	+	+	+	+	+
73 +●	+	+	+	+	+	+	+	+	+	+	+
74 +●	+	+	+	+	+	+	+	+	+	+	+
84 +●	+	+	+	+	+	+	+	+	+	+	+
85+●	+	+	+	+				+	+	+	+
90 +●	+	+	+	+	+	+	+	+	+	+	+
92 +●	+	+	+	+	+	+	+	+	+	+	+
95+●	+	+	+	+	+	+		+	+	+	
109 +●	+	+	+	+	+	+	+	+	+	+	+
112 +	+	+	+	+	+	+	+	+	+	+	+

Table A2: Continued...

117 +	+	+	+	+	+	+	+	+	+	+	+
118 +●	+	+	+	+	+	+	+	+	+	+	+
123+	+		+	+	+	+		+	+		+
128 +●	+	+	+	+	+	+	+	+	+	+	+
129 +	+	+	+	+	+	+	+	+	+	+	+
144 +●	+	+	+	+	+	+	+	+	+	+	+
Nodes of set N_0											
1											
2											
4											
5 +●	+	+	+	+	+	+	+	+	+	+	+
6 +●	+	+	+	+	+	+	+	+	+	+	+
8 +●	+	+	+	+	+	+	+	+	+	+	+
10						+					
12											
13											
19						+					
29							+				
30											
33											
34					+	+					
35										+	
36+	+	+	+	+	+	+	+	+	+		
37							+				+
40											
42											
44 +●	+	+	+	+	+	+	+	+	+	+	+
46 +●	+	+	+	+	+	+	+	+	+	+	+
47 ●										+	+
49										+	+
53											
56											
57+●	+	+	+	+	+	+	+	+	+	+	+
60 +●	+	+	+	+	+	+	+	+	+	+	+
62											+
72			+							+	+
75 +●	+	+	+	+	+	+	+	+	+	+	+
76											
77											
81					+	+					
83											
89											

Table A2: Continued...

91						+					
94+●	+	+	+	+	+	+	+	+	+	+	
96											
98											
99+	+	+	+	+	+	+	+	+	+		
101 +	+	+	+	+	+	+	+	+	+	+	+
102 +●	+	+	+	+	+	+	+	+	+	+	+
104+●	+	+	+	+	+	+	+	+	+	+	
105+●	+	+	+	+	+	+	+	+	+	+	
107											
108+	+	+	+	+	+	+	+	+	+	+	
110					+	+					+
111+●	+	+	+	+	+	+	+	+	+	+	+
114											
115											
116 +●	+	+	+	+	+	+	+	+	+	+	+
124 +●	+	+	+	+	+	+	+	+	+	+	+
125 +●	+	+	+	+	+	+	+	+	+	+	+
126 +●	+	+	+	+	+	+	+	+	+	+	+
131+●	+	+	+	+	+	+	+	+	+	+	
132 +●	+	+	+	+	+	+	+	+	+	+	+
133 +●	+	+	+	+	+	+	+	+	+	+	+
134 +●	+	+	+	+	+	+	+	+	+	+	+
135 +●	+	+	+	+	+	+	+	+	+	+	
137						+				+	
138+	+	+	+	+	+	+	+	+	+	+	
139											
140											
143						+					
145+	+	+	+	+			+	+	+	+	+
146											
Nodes of set X											
3											
7											
9											
14											
15											
16											
17											
18+●	+	+	+	+	+	+	+	+	+	+	
20											

Table A2: Continued...

21											
22											
23											
24											
25 +●	+	+	+	+	+	+	+	+	+		
28											
31											
32 +●	+	+	+	+	+		+	+	+	+	
38											
39											
41+	+	+	+	+	+	+	+	+	+	+	+
48											
50 +●	+	+	+	+	+	+	+	+	+	+	+
52 +●	+	+	+	+	+	+	+	+	+	+	+
54											
55											
58 +●	+	+	+	+	+	+	+	+	+	+	+
63 +	+	+	+	+	+	+	+	+	+		
64											
65 +	+	+	+	+	+	+	+	+	+		
66 +	+	+	+	+	+	+	+	+	+		+
67 +	+	+	+	+	+	+	+	+	+		+
68 +	+	+	+	+	+	+	+	+	+		+
69 +	+	+	+	+	+	+	+	+	+	+	+
71			+							+	+
78											
79											
80 +●	+	+	+	+	+	+	+	+	+	+	+
82+	+	+	+	+	+	+	+	+	+		+
86 +	+	+	+	+	+	+	+	+	+	+	+
87+	+	+	+	+	+	+	+	+	+		+
88+	+	+	+	+	+	+	+	+	+		+
93+	+	+	+	+	+	+	+	+	+	+	+
97		+	+								
100											
103+●	+	+	+	+	+	+	+	+	+	+	
106+●	+	+	+	+	+	+	+	+	+	+	+
113+	+	+	+	+	+	+	+	+	+	+	
119 +	+	+	+	+	+	+	+	+	+	+	+
120 +	+	+	+	+	+	+	+	+	+	+	+
121 +●	+	+	+	+	+	+	+	+	+	+	+

Table A2: Continued...

122						+				+	+
127+●	+	+	+	+	+	+	+	+	+	+	
130+●	+	+	+	+	+	+	+	+	+	+	
136 **+●**	+	+	+	+	+	+	+	+	+	+	+
141											
142+	+	+	+	+	+	+	+	+	+		+

Note:

+ - Nodes recognized to be potential for M ≥ 6.0;

● - Nodes recognized to be potential for M ≥ 6.5;

If an object changes its classification in an experiment, then a relevant cell is shaded;

Numbers of nodes recognized to be potential for M ≥ 6.0 in all experiments are given by bold-italic.